PHYSICAL REVIEW B, VOLUME 64, 241304(R)

Defect-induced nonpolar-to-polar transition at the surface of chalcopyrite semiconductors

John E. Jaffe
William R. Wiley Environmental Molecular Sciences Laboratory Pacific Northwest National Laboratory, Richland, Washington 99352

Alex Zunger
National Renewable Energy Laboratory, Golden, Colorado 80401

(Received 9 May 2001; published 29 November 2001)

In zinc-blende semiconductors, the *nonpolar* (110) surface is more stable than all polar surfaces because the formation of the latter requires the creation of charge-neutralizing but energetically costly surface reconstruction. Our first-principles calculations on $CuInSe_2$ reveal this in the double-zinc-blende (chalcopyrite) structure, the defect-induced reconstructions make the (112)-cation plus $(\overline{112})$-anion polar facets lower in energy than the nonpolar (110) plane, despite the resulting increased surface area. We show that this spontaneous facetting results from the remarkable stability of surface defects (Cu vacancy, Cu-on-In antisite) in chalcopyrites, and explains the hitherto puzzling formation of polar microfacets when one attempts to grow epitaxialloy a nonpolar chalcopyrite surface.

DOI: 10.1103/PhysRevB.64.241304 PACS number(s): 61.72.Ji, 68.35.Bs, 68.35.Md

Chemisorption, catalysis, film growth, and carrier transport on the surfaces of compound semiconductors (GaAs, InP, ZnSe,...,) depend on the atomic structure of the surface.[1–4] Covalently bonded semiconductor surfaces fall into two basic types: nonpolar and polar. In nonpolar zinc-blende surfaces such as (110) there are equal numbers of cations and anions on the surface, so it is charge neutral. Such surfaces do not reconstruct, exhibiting instead only small local atomic displacements and orbital rehybridization with respect to the ideal terminated bulk crystal.[5,6] In contrast, polar surfaces such as zinc-blend (001) or (111) exhibit a nominal charge imbalance[7,8] due to deviations at the surface from the atomic stoichiometry characterizing the underlying bulk solid. This nonzero surface charge density would lead to an ''electrostatic catastrophe,'' [9] i.e., to a divergence of the surface energy. In actuality, semiconductors with polar surfaces avoid this situation by neutralizing their polar surface charge via the creation of reconstruction patterns[1,2] involving the formation of surface defects.[8–10] For example, many anion-terminated zinc-blende (001) and (111) surfaces undergo a (2×4)- or (2×2)-ordered vacancy reconstruction whereby every fourth surface site becomes vacant. While such massive atomic rearrangements do create the needed surface charge neutrality, they are significantly costly in energy, as covalently bonded structures are usually resistant to vacancy formation. Consequently, in all zinc-blende semiconductors investigated, the (110) surface is usually the lowest in energy and is always stable against the formation of polar facets.[1–3,11] Indeed, (110) is the natural cleavage plane of such materials, whereas technological utilization of polar (001) or (111) surfaces requires artificial cutting of the samples. The stability of the zinc-blende (110) surface relative to any combination of ideal or reconstructed polar surfaces is also found in first-principles calculations,[11] as illustrated in Fig. 1(a) for GaAs: We see that the energy of the (110) surface (per area equivalent to that of the polar surfaces) is at least $\sim$2 eV lower than the energy of polar surfaces. The greater intrinsic stability of nonpolar vs. polar surfaces of fourfold-coordinated semiconductors has important implications for facetting chemisorption,[4] catalysis,[4] and film growth, e.g., the preferred surface for film growth[1] on a substrate is the more reactive (001) face, whereas the lower-energy (110) surface leads to poor film growth due to the ease of forming antisite bonds. Thus understanding and controlling the relative stability of polar vs. nonpolar faces could be important in semiconductor material science. Could the polar vs. nonpolar surface stability be reversed in systems where charge-neutralizing defects are easily formed? In this respect an interesting family of candidate semiconductors are the $A^{\mathrm{I}}B^{\mathrm{III}}X_2^{\mathrm{VI}}$ chalcopyrites[12,13] with A^{I}=Cu,Ag B^{III}=Al,Ga,In, and X^{VI}=S,Se,Te. Just like the II-VI or III-V binary zinc-blende semiconductors, chalcopyrites semiconductors are fourfold-coordinated adamantine structures,[12] except that instead of having a single-cation-type II-VIs (e.g., $ZnZnSe_2$), chalcopyrites have two cation types from the neighboring columns in the Periodic Table (e.g., $CuGaSe_2$). This generalization of the binary zinc-blende structure—the availability of two, rather than one type of metal atom—leads in chalcopyrites to easily formed defects.[14] For example, Cu vacancy is nearly exothermic as is the complex between two negatively charged Cu vacancies ($2V_{\mathrm{Cu}}$) and positively charged In-on-Cu antisite ($\mathrm{In_{Cu}}$) in $CuInSe_2$. How would the greater propensity for defect formation affect the polar vs. nonpolar surface stability? It turns out that while there are calculations on *bulk defects*[14] in chalcopyrites, as well as a calculation on defect-free *ideal chalcopyrite surface*,[15] no calculations are available on surface defects in chalcopyrite semiconductors. We performed such pseudopotential LDA calculations, finding that the polar surface of $CuInSe_2$ is considerably more stable than the nonpolar surface, thus reversing the commonly accepted order of stability in binary semiconductors.[1–4] We predict the polar (112) surface to be stabilized by Cu vacancies (V_{Cu}) in Cu-poor conditions, and by Cu-on-In antisite defects $\mathrm{Cu_{In}}$ in In-poor conditions, $(\overline{112})$ is stabilized by subsurface $\mathrm{In_{Cu.}}$ This explains the hitherto puzzling spontaneous formation of microfacets of polar surfaces when one attempts to grow a nonpolar chalcopyrite surface.[16]

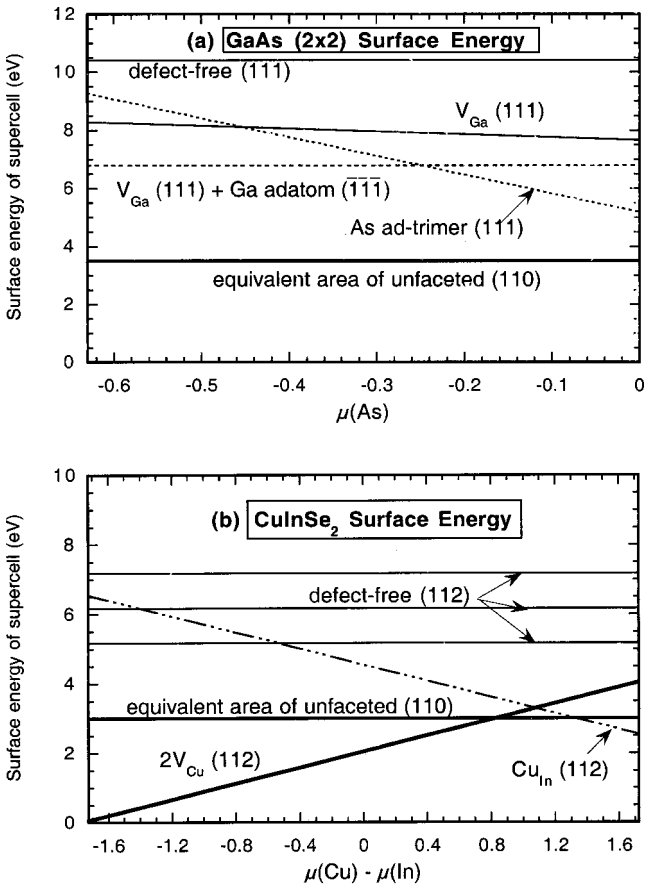

FIG. 1. Surface formation energies vs chemical potential for equivalent slab-supercells of GaAs (Ref. 11) and $CuInSe_2$ (present work). Each curve corresponds to a particular combination of ordered-defect reconstructions on the top and bottom; where only the anion or cation reconstruction is indicated, the opposite face is defect-free. The competing energy of the nonpolar (110) surface is also indicated, and corresponds to an area of (110) that would lie underneath the facets that terminate the polar cell, in the sense shown in Fig. 2. The three ''defect free'' lines in (b) correspond to different gap corrections (see text).

Geometry: In $CuInSe_2$(CIS) the nonpolar (110) surface [also called (220)] has zigzag chains of atoms Cu-Se-In-Se,..., each atom having two surface bonds, one dangling bond into the vacuum, and one back bond pointing to the second atomic layer. In the limit of identical cations, this surface reverts to zinc-blende (110). In contrast, the ideal-cation (112) and $(\bar{1}\bar{1}2)$-anion polar surfaces of CIS have four threefold-coordinated terminal atoms per rectangular primitive surface unit cell. In the limit of identical cations this would revert to a perfect triangular 2D lattice with one atom per cell at each (111) and $(\bar{1}\bar{1}\bar{1})$ surface. Figure 2 shows the geometrical relation between polar (110) and nonpolar (112) and $(11\bar{2})$ [crystallographically equivalent to $(\bar{1}\bar{1}2)$] faces. The latter makes angles of about 35° with the substrate plane and 109° with each other. The formation of these ridges increases the surface area over a (110) planar surface by a factor of $[1+c^2/(8a^2)]^{1/2}=\sec(35.4°)=1.227$, where a and c are the chalcopyrite lattice constants.

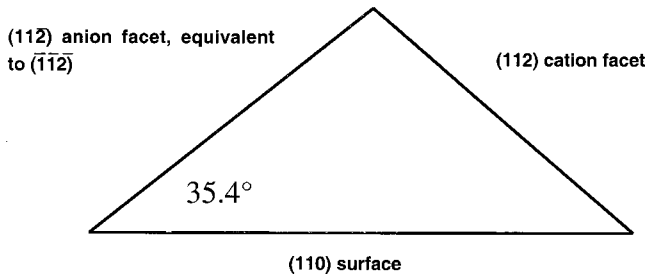

FIG. 2. Side view of prism-shaped ridge covering the macroscopic (110) nonpolar plane of $CuInSe_2$, bounded by facets of the cation-terminated (112) surface and its Se-terminated counterpart.

Method: We performed bulk and slab-supercell surface total energy calculations on CIS using the local density approximation[17] (LDA) and the ultrasoft-pseudopotential[18] plane-wave total energy method,[19] as implemented by the VASP code.[20] Since charge transfer can create a metallic state at polar surfaces, Fermi surface smearing[21] was used for accurate k-space integration. Relatively high precision settings were used, with a target accuracy[22] in the total energy of about 1 meV/atom in bulk calculations and 10 meV per surface atom for surface energies. We obtained bulk CIS lattice constants $a=5.693$ Å and $c=11.441$ Å, a ratio $c/a=2.0097$, and anion sublattice parameter[13] $u=0.2173$. These lattice constants are about 1.5% smaller than the experimental[13] values $a=5.784$ Å and $c=11.616$ Å, as is typical for the LDA, while the dimensionless numbers are very close to experiment ($c/a=2.0083$ and[23] $u=0.224$). Since we are considering reconstructions that change the system's chemical composition, we compared the surface formation energies in a grand canonical formulation. Defining the chemical potential for each element relative to its pure bulk phase, and setting $\mu_{Se}=0$ (since we do not consider Se vacancies), we write the surface formation energy for one unit cell of our polar slab as

$$\Delta H_f=\Delta E+n_{Cu}\mu_{Cu}+n_{In}\mu_{In}, \tag{1}$$

where

$$\Delta E=E_{surface}-NE_{bulk}+n_{Cu}E_{bulk}(Cu)+n_{In}E_{bulk}(In). \tag{2}$$

Here $E_{surface}$ is the total energy of the surface-containing supercell, and NE_{bulk} is the energy of an equivalent amount of bulk CIS. n_{Cu} and n_{In} are the numbers of Cu and In atoms *removed* from the ideal unit cell to create the defects, if any; their respective values are -1 and $+1$ for the Cu_{In} cell, and $+2$ and 0 for the $2V_{Cu}$ cell. When we substitute the appropriate computed bulk and surface energies, we obtain

$$\begin{aligned} 2V_{Cu}: &\quad \Delta H_f=3.78\,\text{eV}+2\mu_{Cu},\\ Cu_{In}: &\quad \Delta H_f=4.55\,\text{eV}-\mu_{Cu}+\mu_{In},\\ \text{Defect-free}: &\quad \Delta H_f=5.2-7.2\,\text{eV}. \end{aligned} \tag{3}$$

The range of values for the defect-free slab reflects possible effects of LDA band-gap errors: A polar slab depolarizes itself by moving valence charges from the anion surface into conduction bands associated with the cation surface, and the energy cost of doing this should scale with the band gap. One possible correction for this would be to increase the supercell energy by the number of electrons transferred (two) times the difference between the computed and experimental bulk gaps, giving about 2 eV. For a second estimate, we calculated the ideal energies of the (110) and (111)/$(\overline{111})$ surfaces of several zinc-blende II-VI semiconductors, extracted a component of the polar-nonpolar surface energy difference that scaled with the LDA band gap, then rescaled this component by shifting the gap to its experimental value, yielding a correction of about 1 eV in CIS. These error estimates were included in our results below.

The Nonpolar (110) Surface of $CuInSe_2$: We used a five-layer slab in which the top three atomic layers were allowed to relax and the bottom two were held fixed, with the number of vacuum layers equal to the number of occupied layers. Test calculations on thicker slabs showed only negligible changes in surface energy. We find that when fully relaxed, the CIS (110) surface assumed a structure typical of nonpolar surfaces in zinc-blende compound semiconductors:[5,6] The top layer developed a large bond rotation in which the surface cations sank into the slab and the anions rose outwards. We generalized the usual coordinates used to define such relaxations[5] by defining separate rotation angles for the two distinct surface cations with respect to an average position of the two surface anions, obtaining $\omega_{\mathrm{Cu}}=36.1°$ and $\omega_{\mathrm{In}}=38.7°$. These surface rotation angles are larger than in typical II-VI and III-V compounds ($25°<\omega<33°$) and approach those seen in experimental studies of the CuCl (110) surface (41.3° and 44.1°, respectively.)[24] These large rotation angles reflect the greater ionic character in CIS relative to the III-Vs and II-VIs. Bonds in the second atomic layer of the CIS (110) slab rotate by about −6° while those in the third layer rotate from the plane of the slab by less than 1°. The surface layer bonds contracted by an average of about 2.5% on relaxation. The unrelaxed and fully relaxed surface energies are 0.617 and 0.376 eV per average surface atom, or 0.859 and 0.523 J/m^2, respectively.

The Cation-Terminated (112) and Anion-Terminated $(\overline{112})$ Polar Surfaces of $CuInSe_2$: Each slab supercell has a cation-terminated (top) (112) face, and an anion-terminated $(\overline{112})$ (bottom) face. For the anion-terminated $(\overline{112})$ bottom face we consider only the defect-free, *p*-type metallic case. For the top (112) face we consider the point defects that have been previously identified[14] in bulk CIS which can neutralize this surface: (i) the $\mathrm{Cu_{In}}$ antisite (one per four-atom surface unit cell) under Cu-rich conditions; (ii) the Cu vacancy (two per surface cell) under Cu-poor conditions; (iii) the defect-free cation face, *n*-type which is metallic. Each of the three slabs (i)–(iii) so defined has ten atomic layers and four atoms per layer, with the inner two layers frozen at the computed bulk geometry and the top [(112)] four and bottom [$(\overline{112})$] four fully relaxed. In the $\mathrm{Cu_{In}}$ antisite case (i), relaxations were in the *z* direction, −0.17 Å for the three surface Cu atoms and −0.22 Å for the surface In, making the surface cations approximately coplanar with the top layer of anions. In the $2V_{\mathrm{Cu}}$ case (ii) of two Cu vacancies, the top In atoms are displaced downwards by 0.16 Å making them almost coplanar with the top Se layer. There is also a displacement of about 0.03 Å of the neighboring Se atoms towards the Cu vacancies. In all cases there were only slight displacements of the bottom (anion) surface atoms from their bulk positions. The In atoms in the layer just above the bottom relaxed downwards by about 0.01 Å in each case, and all other displacements in the bottom half of the slab were less than 0.005 Å. The energy change per unit cell due to geometric relaxation was −2.267 eV for the antisite cell (i), −1.594 eV for the Cu vacancy cell (ii) and −0.928 eV for the defect-free cell (iii).

Stability of Polar vs. Nonpolar Surfaces: Figure 1(b) compares the energies of polar and nonpolar CIS surfaces vs. the chemical potential difference $\mu_{\mathrm{Cu}}-\mu_{\mathrm{In}}$, extending from Cu poor (left) to In poor (right). We plotted these formation energies along the Se-rich stability line $\mu_{\mathrm{Se}}=0$, noting that along this line $\mu_{\mathrm{Cu}}+\mu_{\mathrm{In}}$ is constrained to equal our calculated CIS heat of formation (−1.725 eV per formula unit) since $\mu_{\mathrm{Cu}}+\mu_{\mathrm{In}}+2\mu_{\mathrm{Se}}$ must always equal that quantity in chemical equilibrium. As noted above (*viz.* Fig. 2), the combined surface energies of the top and bottom faces of the polar slabs [which equal the surface formation energy of Eq. (1)] should be compared with the energy of an area of the nonpolar (110) surface that is 1.227 times smaller. Using the relaxed (110) surface energy density of 0.523 J/m^2, the equivalent (110) surface energy is thus 3.00 eV. Figure 1(b) shows that (a) the *defect-free* polar (112)/$(\overline{112})$ facets are much higher in energy than the nonpolar (110) surface, as is the case in binary semiconductors [*viz.* Fig. 1(a)]. Similarly, Wander *et al.*,[25] recently found that in ZnO the surface energy density for the average of the defect-free anion-terminated plus cation-terminated polar surfaces about 1.7 times higher than that of the simplest nonpolar surface. This is comparable to the ratio we found in CIS (1.4–2.0, depending on the band-gap correction). However, the (b) introduction of ordered-defect reconstruction in CIS lowers the surface formation energy of the polar (112)/$(\overline{112})$ below that of the nonpolar (110) over most of the attainable composition range, making the (110) surface thermodynamically unstable with respect to (112)/$(\overline{112})$ facet formation. When defects at the $(\overline{112})$ surface (such as Cu adatoms or $\mathrm{In_{Cu}}$ in the next layer up), are energetically favored then they will lower the free energy of the polar facets even more, compared to the unfaceted (110) surface (Wander *et al.*,[25] gave experimental evidence that in ZnO the anion surface really is defect-free).

Our main finding that polar surfaces in chalcopyrites are defect-stabilized to an extent that makes them thermodynamically preferred over the nonpolar surface has a number of important implications: First, this explains the previously puzzling result that the chalcopyrite cleavage plane is the polar face.[26] Second, this explains the remarkable spontane-

ous formation of $(112)+(\overline{1}\overline{1}2)$ microfacets of epitaxial polar surfaces, as shown schematically in Fig. 2, when one attempts to grow nonpolar surfaces.[16] Both results reflected the intrinsic thermodynamic stability of the polar surfaces. Third, our result might explain the dramatic reduction in free-carrier density observed when growing the nominally nonpolar chalcopyrite surface that reverts to $(112)+(\overline{1}\overline{1}2)$ polar microfacets:[16,27] The conditions for electrostatic stability require the surface defects considered here to be fully ionized, since otherwise they would not accomplish the needed charge neutralization of the polar surfaces. In particular, the electrostatic potential pushes the valence band up until it overlaps the acceptor defects at the (112) surface, ionizing them and releasing holes. These holes however do not provide free carriers within the bulk of the sample, as they are confined electrostatically at or near the anion surface. If the latter also has an ordered-defect reconstruction involving donors such as anion vacancies, these will exactly compensate the holes from the cation surface. In either case, the polar-faceted nonpolar plane is autocompensated by the equal areas of anion and cation facets leading to the observed dramatic decrease in carrier density. Finally, we note that the insights gained here on the crucial role of introduction of low formation energy defects in reversing polar vs. nonpolar stability may be helpful in designing polar-stable zincblende structures via addition of suitable cation elements.

In summary, we have shown that our calculation explains the remarkable nonpolar-to-polar surface faceting transition observed[16,26] in chalcopyrite semiconductors. The defect-free polar surface has a well-defined metallic[11] electronic structure, but with too high a formation energy to compete with the nonpolar surface. The analogous surface reconstruction in binary zinc-blende semiconductors is energetically unfavorable[11] by a wide margin for any combination of surface defects and at any attainable chemical potential. This reflects the higher energy of all the native point defects available in binary compounds. The unique structure of chalcopyrite polar surfaces is likely to have important consequences for their electrical properties, including possible surface autocompensation due to the equal areas of anion and cation facets.

The authors acknowledge useful discussions with A. Rockett on his unpublished experimental results (Ref. 16). J.E.J. acknowledges the support of the Laboratory Directed Research and Development program, Pacific Northwest National Laboratory. operated for the U.S. Department of Energy by Battelle Memorial Institute under Contract No. DE-AC06-76RLO1830. A.Z.'s work at NREL was supported by the U.S. Department of Energy, EERE Grant No. DE-AC36-98-GOL0337.

[1] W. Monch, in *Semiconductor Surfaces and Interfaces*, Vol. 16 of Springer Series in Surface Science (Springer, Berlin, 1995).
[2] M. Lannoo and P. Friedel, in *Atomic and Electronic Structure of Surfaces*, Vol. 16 of Springer Series in Surface Science (Springer, Berlin, 1991).
[3] F. Bechstadt and R. Enderlein, *Semiconductor Surfaces and Interfaces* (Akademie-Verlag, Berlin, 1988).
[4] R. Hoffman, *Solids and Surfaces* (VCH Publishers, New York, 1988).
[5] J. P. LaFemina, Surf. Sci. Rep. **16**, 133 (1992).
[6] C. B. Duke, in *Reconstructions of Solid Surfaces*, edited by K. Christman and K. Heinz (Springer, Berlin, 1990).
[7] C. Noguera, J. Phys.: Condens. Matter **12**, R367 (2000).
[8] M. D. Pashley, Phys. Rev. B **40**, 10 481 (1989).
[9] W. Harrison, *Electronic Structure and Properties of Solids* (Freeman and Co., San Francisco, CA, 1980), p. 229.
[10] S. Froyen and A. Zunger, Phys. Rev. Lett. **66**, 2132 (1991).
[11] N. Moll, A. Kley, E. Pehlke, and M. Schaffer, Phys. Rev. B **54**, 8844 (1996). At the very anion rich conditions, an anion trimer reconstruction of the $(\overline{1}\overline{1}1)$ face can be lower in energy per unit area than the (110), but when formed from (110) its surface area triples. Consequently, in III-V, the (110) face is always present as equilibrium crystal shape.
[12] E. Parthe, *Crystal Chemistry of Tetrahedral Structures* (Gordon and Breach, New York, 1964).
[13] J. L. Shay and J. H. Wernick, *Ternary Chalcopyrite Semiconductors* (Pergamon, Oxford, 1975).
[14] S. B. Zhang, S. H. Wei, and A. Zunger, Phys. Rev. Lett. **78**, 4059 (1997).
[15] J. A. Rodriguez, L. Quiroga, A. Camacho, and R. Baquero, Phys. Rev. B **59**, 1555 (1999).
[16] D. Liao and A. Rockett, in Proceedings of the 28th IEEE Photovoltaic Specialists Conference, Anchorage, AK, Sept. 15–22, 2000 (Institute of Electrical Engineers, New York, 2001, in press).
[17] W. Kohn and L. J. Sham, Phys. Rev. **104A**, 1133 (1965).
[18] J. D. Vanderbilt, Phys. Rev. B **41**, 7892 (1990).
[19] J. Ihm, A. Zunger and M. L. Cohen, J. Phys. C **12**, 4409 (1979).
[20] G. Kresse and J. Hafner, Phys. Rev. B **47**, 558 (1993); Phys. Rev. B **48**, 13 115 (1993).
[21] M. Methfessel and A. T. Paxton, Phys. Rev. B **40**, 3616 (1989).
[22] For bulk CIS, we used 196 *k* points in the irreducible Brillouin zone and a energy cutoff of 17.18 Ry. Geometry relaxation was stopped when the energy changed by less than 1 meV corresponding to a maximum atomic force of about 0.03 eV Å.
[23] H. W. Spiess, v. Haeberlin, G. Brandt, A. Rauber, and J. Schneider, Phys. Status Solidi A **62**, 183 (1974).
[24] A. Kahn, S. Ahsan, W. Chen, M. Dumas, C. B. Duke, and A. Paxton, Phys. Rev. Lett. **68**, 3200 (1992).
[25] A. Wander *et al.*, Phys. Rev. Lett. **86**, 3811 (2001).
[26] Z. A. Shukri and C. H. Champness, Surf. Rev. Lett. **5**, 419 (1998); Acta Crystallogr., Sect. B: Struct. Sci. **53**, 620 (1997).
[27] M. A. Contreras, B. Egaas, D. King, A. Swartzlander, and T. Dullweber, Thin Solid Films **361-362**, 167 (2000).